

SCIENTIFIC REPORTS



OPEN

Orthogonality of Pyrrolysine tRNA in the *Xenopus* oocyte

Daniel T. Infield, John D. Lueck, Jason D. Galpin, Grace D. Galles & Christopher A. Ahern 

Chemical aminoacylation of orthogonal tRNA allows for the genetic encoding of a wide range of synthetic amino acids without the need to evolve specific aminoacyl-tRNA synthetases. This method, when paired with protein expression in the *Xenopus laevis* oocyte expression system, can extract atomic scale functional data from a protein structure to advance the study of membrane proteins. The utility of the method depends on the orthogonality of the tRNA species used to deliver the amino acid. Here, we report that the pyrrolysyl tRNA (*pylT*) from *Methanosarcina barkeri fusaro* is orthogonal and highly competent for genetic code expansion experiments in the *Xenopus* oocyte. The data show that *pylT* is amendable to chemical acylation *in vitro*; it is then used to rescue a cytoplasmic site within a voltage-gated sodium channel. Further, the high fidelity of the *pylT* is demonstrated via encoding of lysine within the selectivity filter of the sodium channel, where sodium ion recognition by the distal amine of this side-chain is essential. Thus, *pylT* is an appropriate tRNA species for delivery of amino acids via nonsense suppression in the *Xenopus* oocyte. It may prove useful in experimental contexts wherein reacylation of suppressor tRNAs have been observed.

The method of *in vivo* nonsense suppression in *Xenopus laevis* oocytes via chemically aminoacylated tRNA has enabled the site-specific encoding of over 100 different amino acids into ion channels and other proteins^{1–3}. This expression system is advantageous because the oocyte faithfully manufactures and traffics diverse ion channel and receptor proteins, where established techniques allow their analysis from the macroscopic to the level of single proteins. Noncanonical amino acids (ncAAs) have allowed atomic-level insights into structure, function, and pharmacology of ion channels. The system's flexibility arises from the facile attachment of dinucleotide-amino acid substrates to truncated tRNA via enzymatic ligation⁴. That is, the same species of tRNA can be used for encoding the amino acid needed for the experimental inquiry, in contrast to co-injecting an aminoacyl-tRNA synthetase for ncAA aminoacylation^{5–7}. For this reason, chemical acylation of tRNAs is widely used for genetic code expansion in *Xenopus* oocytes.

This approach continues to be useful for obtaining high-resolution functional details from a variety of ion channel and receptors. Notable examples of its use on post-synaptic ligand gated channels include the advancing of the energetic basis for ligand recognition^{8,9}, main-chain chemistry in channel gating¹⁰, protein thermodynamics in channel activation⁹; as well as the application to voltage-gated ion channels^{11–17}.

Multiple tRNA species have been used for delivery in the oocyte system, the most common being a mutated version of the glutamine tRNA from *Tetrahymena thermophila*, commonly termed THG73¹⁸. The utility of this tRNA is derived from the fact that it is a natural amber (TAG) suppressor, therefore eliminating the need to alter the anticodon for nonsense suppression application. The specific motivation for the G73 mutation was to obscure recognition of the THG73 tRNA by endogenous glutamine synthetases in the oocyte expression system, thus increase its orthogonality. Although THG73 is orthogonal, multiple groups including ours have reported that it is susceptible under some experimental conditions to reacylation by endogenous glutaminyl-tRNA synthetases^{19–22}. Efforts to further mutate THG73 to increase orthogonality have only been partially successful and are unable to completely eliminate *in situ*. The potential “error” introduced by tRNA reacylation is significant. Depending on the functional tolerance at the site of incorporation within the target protein, misincorporation may lead to a mixed population of glutamine and the ncAA at the encoding site (introduced stop codon, usually TAG; amber codon)^{19,20}. This variability can be controlled for by careful analysis of conditions performed in parallel with non-acylated tRNA (tRNA-CA), varied length of incubation following injection and limited abundance of tRNA, which provides an experimental window in which ncAA rescue precedes any such unintended readthrough event. However, if such an experimental window cannot be found, the encoding site must be abandoned²².

Department of Molecular Physiology and Biophysics, Iowa Neuroscience Institute, University of Iowa, Iowa City, IA, 52242, USA. Daniel T. Infield and John D. Lueck contributed equally to this work. Correspondence and requests for materials should be addressed to C.A.A. (email: christopher-ahern@uiowa.edu)

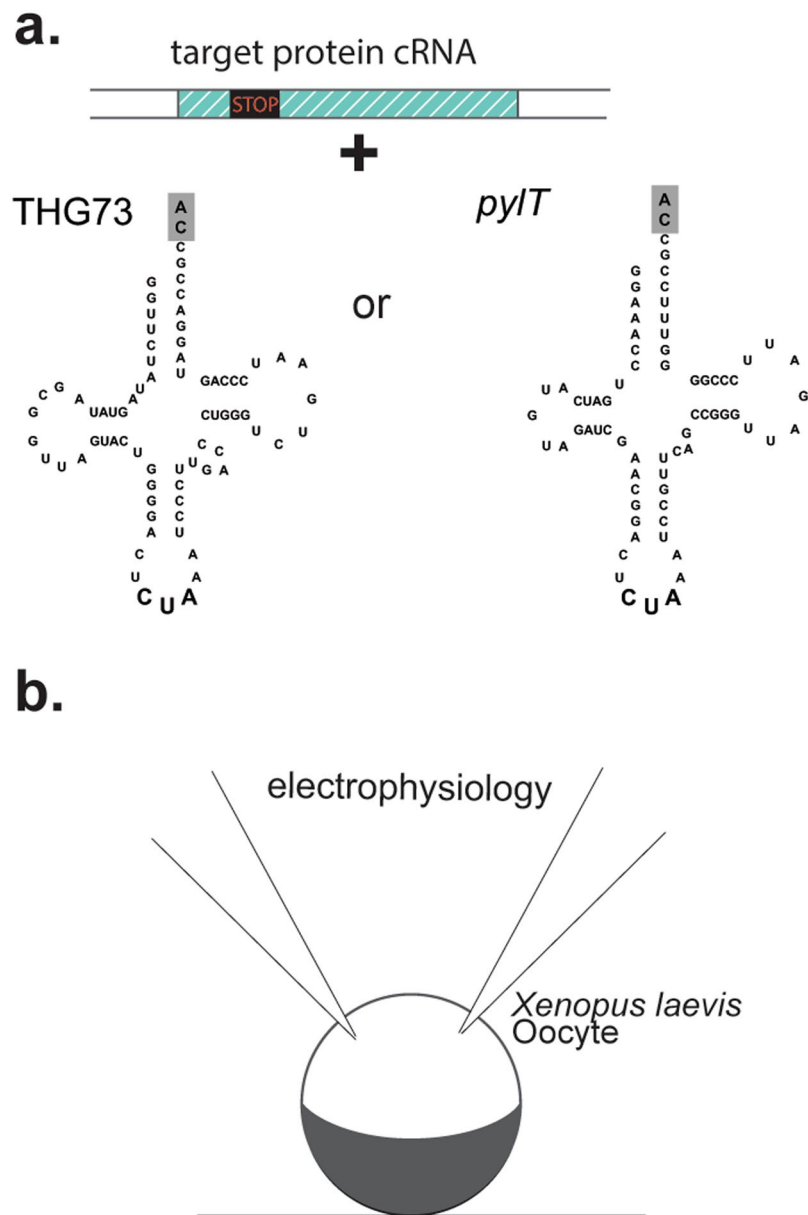


Figure 1. Misacylation of orthogonal tRNA for genetic code expansion. **(a)** Target protein cRNA containing a site-directed stop codon (nonsense codon) is subsequently suppressed by an orthogonal tRNA - THG73 or pyrrolysine tRNA (*pylT*). The grey highlighted nucleotides “CA” represent ligated pdCpA (see methods). **(b)** Co-injection of tRNA and cRNA into the *Xenopus* oocyte enables electrophysiological two-electrode voltage clamp characterization of ion channels and receptors containing ncAA.

Pyrrolysine, the so-called “22nd amino acid,” is encoded by methanogenic archaea and bacteria using a tRNA that naturally recognizes the amber codon TAG^{23,24}. This unique tRNA (*pylT*) displays exceptional orthogonality in bacteria and in mammalian cells and has been used to encode ncAAs via evolved aminoacyl-tRNA synthetases that recognize an amino acid of interest²⁵. Overall, tRNA-synthetase pairs have enabled the encoding of more than 100 ncAAs in diverse environments including cell free translation^{17,26}, mammalian cells²⁷, bacteria²⁸, and even whole animals²⁹. However, the evolution of aminoacyl-tRNA synthetases to discern derivatized isosteric analogs from their natural amino acids counterparts (often necessary for atomic-level insights) has proven challenging. Here, we assayed the orthogonality of *pylT* via *in vitro* chemical aminoacylation and injection into *Xenopus* oocytes (Fig. 1), using high-resolution ion channel function as a sensitive and quantitative readout of rescue and readthrough.

Results

The sodium channel conducting state is strongly coupled to the transmembrane potential, thus one can precisely measure the flow of sodium conductance through the channel through standard electrophysiological approaches, Fig. 1. Voltage-gated sodium channel activation is characterized by transient inward, rapidly inactivating ionic

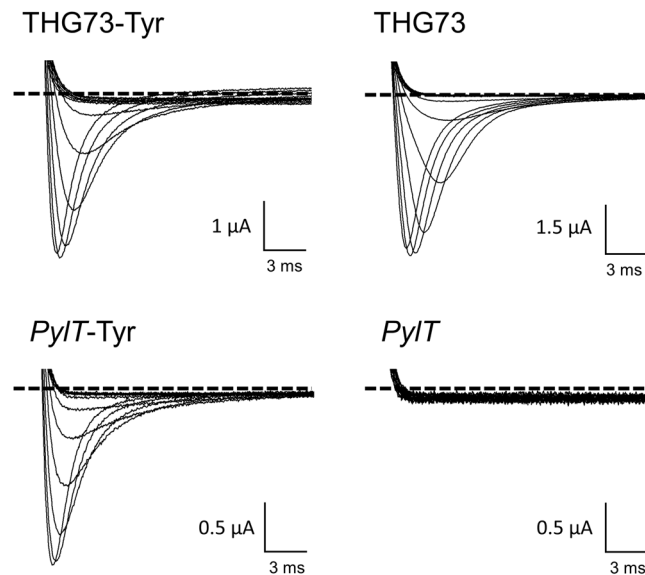


Figure 2. Rescue of an introduced stop codon into the human cardiac voltage gated sodium channel. Voltage-induced currents upon co-injection of hNav_v 1.5 S571TAG with either acylated (left) or unacylated tRNA (right) variants THG73 (top) or *pylT* (bottom). *Xenopus* oocytes expressing sodium channel variants were subjected to membrane depolarizations (steps from -80 mV to -20 mV). Traces show development of rapidly inactivating sodium currents as downward deflections. The level of zero current for each cell is indicated by a black dashed line.

Injection condition (24 hr)	Current at -20 mV (μ A)	Std. Deviation	N-value	P-value (vs. like tRNA)
THG73	-3.68	2.36	6	—
THG73-Tyr	-2.26	1.53	5	0.13
<i>pylT</i>	0.011	0.0021	5	—
<i>pylT</i> -Tyr	-1.31	0.44	5	0.0025
S571TAG	-0.0073	0.0065	4	—

Table 1. Quantification of Nav currents of hNav_v1.5-S571TAG when co-injected with THG73 or *pylT* tRNA.

currents. When cells are bathed in physiological recording solutions, e.g. 140 mM extracellular sodium, inward sodium currents appear as downward deflections in response to transient depolarization^{30,31}; thus the level of recorded negative current is directly indicative of the number of full-length functional channels at the cell surface. To begin to scrutinize the orthogonality of the *pylT*, we chose amino acid position S571 in the human cardiac sodium channel hNav_v1.5 as a model site for encoding. Serine 571 is located in an unstructured intracellular loop between two domains of the channel and importantly has been mutated to other amino acids with diverse side-chain chemistries via conventional mutagenesis without compromising channel function³². We co-injected *Xenopus laevis* oocytes hNav_v 1.5 S571 cRNA (complementary RNA generated via *in vitro* transcription) with acylated and non-acylated tRNAs, and measured currents using the Two-Electrode Voltage Clamp technique after 24 hours³³. When THG73 was used as the carrier tRNA for this position, significant hNav_v1.5 current was generated in the presence or absence of an appended tyrosine amino acid (i.e., whether we ligated the pdCpA, which lacks an amino acid, or the pdCpA-Tyrosine substrate) (Fig. 2, top panels). There was, in fact, no significant difference in the two conditions after 24hrs (Table 1), eliminating the prospect of adjusting injection conditions to abrogate readthrough while sparing rescue. Injection of S571TAG hNav_v1.5 cRNA alone did not elicit significant current, signifying that this site lacks appreciable ‘intrinsic’ bleedthrough at the level of the cRNA (Table 1)^{19–21}. Therefore, in these conditions, it is possible that THG73-CA is acylated by an endogenous aminoacyl synthetase, and the resultant acylated tRNA supports the incorporation of an amino acid at position S571. By contrast, co-injection of *pylT* and hNav_v1.5-S571TAG yielded sodium currents that were strictly dependent on tRNA acylation, (Fig. 2, lower panels). Specifically, no sodium currents were detected for the condition for hNav_v1.5-S571TAG with non-acylated *pylT* (*pylT*-CA). In contrast, robust voltage-dependent sodium currents were seen when channel cRNA was co-injected with an tyrosine-acylated *pylT* (*pylT*-Tyr).

To confirm the *in vitro* enzymatic ligation of pdCpA and pdCpA- amino acid substrates to *pylT*, ligated and unligated tRNA samples assayed via denaturing TBE-Urea gels. Ligation of the pdCpA substrate is indicated by a gel shift corresponding to a two nucleotide increase in tRNA length. As indicated in Fig. 3, both pdCpA and pdCpA-amino acid substrates were efficiently ligated by the T4 RNA ligase. Therefore, the lack of observed reacylation-based readthrough in the oocyte expression system was not due to a lack of ligation of the pdCpA dinucleotide to truncated *pylT*.

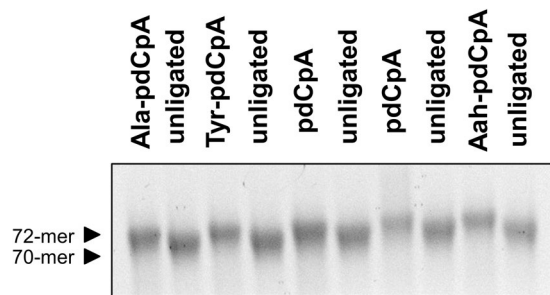


Figure 3. *pylT* can be efficiently ligated to dinucleotide-amino acid substrates *in vitro*. TBE UREA tRNA gels show successful ligation of substrates to *pylT*. Approximately 2 μg of tRNA was run per well. Each lane represents an independent ligation. Note the consistent gel shift representative of ligation of the dinucleotide-amino acid substrate to the truncated *pylT*. Abbreviations: Ala (alanine), Tyr (tyrosine), Aah (alpha-hydroxy alanine). Examples of additional substrate types are available in the Supplementary Figures.

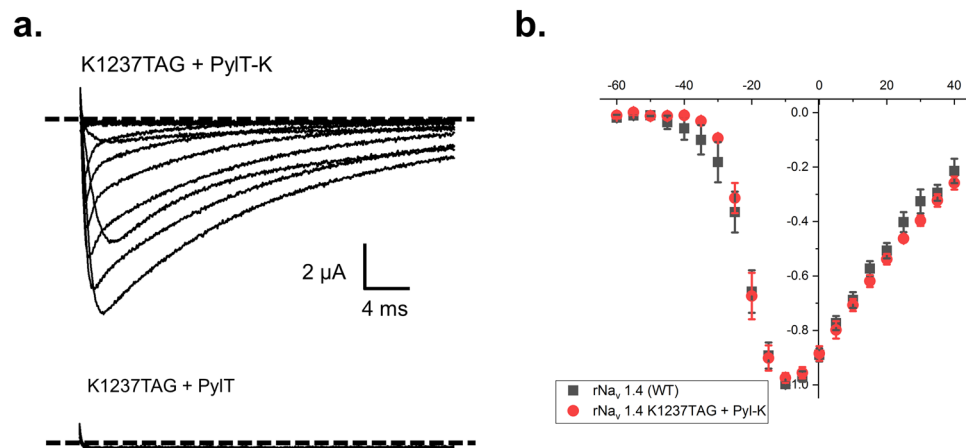


Figure 4. *pylT* enables the faithful encoding of lysine into position K1237 of $r\text{Na}_v 1.4$. **(a)** Example traces of $r\text{Na}_v 1.4$ -K1237TAG cRNA co-injected with either lysine-acylated (top) or unacylated full length (bottom) *PylT*. Oocytes were held at -100 mV and pulsed from -80 mV to $+40$ mV with 30 ms depolarizing steps. Voltage gated sodium channel activity is evidenced by increasingly large downward deflections in the traces in response to depolarization. The level of zero current for each cell is indicated by a dashed line. **(b)** Normalized current-voltage relationship plots comparing the WT $r\text{Na}_v 1.4$ channel to that of the $r\text{Na}_v 1.4$ K1237TAG rescued with lysine.

The encoding fidelity of *pylT* was evaluated independently by rescuing a stop codon at position K1237 which resides in the sodium ion-selectivity filter of the rat skeletal muscle sodium channel, $r\text{Na}_v 1.4$. This unique structural feature promotes the selective passage of sodium through the channel over other monovalent cations, namely potassium. Mutagenesis and functional studies demonstrate that, while this site when mutated produces functional channels, the lysine amino acid at this position is absolutely necessary to support selectivity of sodium ions through the pore^{34,35}. As a consequence of this functional prerequisite, any other amino acid encoded at this site, even the charged congener arginine, results in altered channel selectivity. Using standard electrophysiological approaches, ion channel selectivity can easily be quantified. Altered sodium ion selectivity of $r\text{Na}_v 1.4$ -K1237 is evidenced by a shift in the so-called reversal potential from $+60$ mV, the Nernst potential for sodium, to near 0 mV, the voltage where electrochemical gradients are balanced for a non-selective pore³⁶. To demonstrate the encoding fidelity of the *pylT*, we co-injected $r\text{Na}_v 1.4$ -K1237TAG cRNA and *pylT*-lysine and observed voltage-dependent currents of size -4.9 ± 1.1 μA at -20 mV ($N = 5$) (Fig. 4A). Currents resulting from co-injection of $r\text{Na}_v 1.4$ K1237TAG and full length (pdCpA-ligated) *pylT* were negligible (-0.12 ± 0.13 μA , $N = 10$, Fig. 4B). Importantly, the rescued channels displayed a reversal potential of $+64.6 \pm 3.9$ mV ($N = 5$, Fig. 4). This value is in close agreement with that of WT $r\text{Na}_v 1.4$ recorded in parallel ($+66.6 \pm 2.1$ mV, $N = 4$, $p = 0.72$ between conditions), confirming the strict encoding of lysine at K1237TAG.

Discussion

Taken together, our results demonstrate that *pylT* is orthogonal in the *Xenopus* oocyte, and that it is useful for genetic code expansion experiments. We used voltage-gated sodium channels as exemplar proteins for this purpose, but we have also begun to enlist *pylT* as a tRNA for delivery of ncAAs into voltage-gated potassium channels, chloride channels, and enzymatic pumps, and these efforts have thus far been met with similar results. Thus, *pylT* may be used as an alternative to THG73 in cases where recylation of THG73 poses a significant challenge.

However, regardless of the species being used, we regard it advantageous to test for bleedthrough via co-injection of cRNA of interest with the pdCpA-ligated tRNA as there is no substitute for the empirical support provided by this negative control. It is also highly advantageous that *pylT* has been shown to be amenable to recoding of its anticodon from TAG to TGA and TAA³⁷. Therefore, it may be used in future studies wherein site-specific dual suppression is desired¹⁶. Finally, it bears mentioning that there are additional tRNA species that have been shown to be orthogonal as part of coevolved tRNA- aminoacyl-tRNA synthetase pairs. Two such pairs have been successfully used in *Xenopus* oocytes^{6,7}. These suppressor tRNAs therefore represent good candidates to test for amenability for chemical aminoacylation in future studies.

Methods

Molecular Biology. The S571TAG mutation was made into a pcDNA3.1 human Na_v1.5 construct³⁸ and the K1237TAG mutation was made into a pBSTA-based rat Na_v1.4 construct²² using standard methods. For direct comparison of THG73 and *pylT* in hNa_v1.5, tRNA was generated and purified using the exact same procedure described by our group in detail in a recent report²⁶. The transcription of template oligonucleotides generated tRNA with the following sequences: for THG73:

G G U U C U A U A G U A U A G C G G U U A T U A C U G G G G A C U C U A A A U C C C U U G A C C C -
U G G U C U G A A U C C C A G U A G G A C C G C

for *pylT*:

G G A A C C U G A U C A U G A U G A U C G A A C G G A C U C U A A A U C C G U U C A G C C G G U U A G A U U C C C G G G
G U U U C C G C

For experiments assaying the fidelity of encoding in the selectivity filter of rNa_v1.4, the *pylT* 70mer tRNA was synthesized by Integrated DNA Technologies (Coralville, IA). In all cases tRNA was reconstituted in 10 mM HEPES pH 7.2 and 3 mM MgCl₂ and it was refolded in a thermocycler using a protocol with a denaturation step (94 °C for 3 min), followed by a linear ramp down to 4 °C over 20 minutes. Ligation reaction conditions, purification of acylated tRNA, and reconstitution of acylated tRNA were done as recently described²⁶. Denaturing TBE-Urea gels were run as described in⁴ except that precast Mini-Protean gels were used (Biorad, Hercules CA).

Electrophysiology. *Xenopus laevis* oocytes were obtained through Ecocyte, Inc (Austin TX USA). For rescue of hNa_v1.5 and rNa_v1.4, we injected 25 nl of 1 ng/nl Na_v cRNA and 25 nl of 25 µg of a tRNA pellet resuspended in 2.5 µl 3 mM cold NaOAc. Recordings were made approximately 24 hours later. For Na_v1.5 experiments only, we also injected 12.5 ng of the rat β1 cRNA. For WT Na_v1.4, we injected 2 ng of cRNA and recorded currents 24 hours later. All recordings were in oocyte Ringer's essentially as described previously²². Currents were analysed via Clampfit 9.2, Molecular Devices, (Sunnyvale, CA). Reversal potentials were derived by fitting the linear component of the current-voltage relationship (+20 to +40 mV), and solving for the y-intercept. Statistical analysis was by unpaired student's t-test, and exact p-values are noted in the text or tables.

Data availability. The raw data pertinent to this study is available from the authors upon reasonable request.

References

- Dougherty, D. A. & Van Arnam, E. B. *In vivo* incorporation of non-canonical amino acids by using the chemical aminoacylation strategy: a broadly applicable mechanistic tool. *Chembiochem: a European journal of chemical biology* **15**, 1710–1720, <https://doi.org/10.1002/cbic.201402080> (2014).
- Pless, S. A. & Ahern, C. A. Unnatural amino acids as probes of ligand-receptor interactions and their conformational consequences. *Annual review of pharmacology and toxicology* **53**, 211–229, <https://doi.org/10.1146/annurev-pharmtox-011112-140343> (2013).
- Leisle, L., Valiyaveetil, F., Mehl, R. A. & Ahern, C. A. Incorporation of Non-Canonical Amino Acids. *Advances in experimental medicine and biology* **869**, 119–151, https://doi.org/10.1007/978-1-4939-2845-3_7 (2015).
- Nowak, M. W. *et al.* *In vivo* incorporation of unnatural amino acids into ion channels in *Xenopus* oocyte expression system. *Methods in enzymology* **293**, 504–529 (1998).
- Martin, R. P., Sibley, A. P., Dirheimer, G., de Henau, S. & Grosjean, H. Yeast mitochondrial tRNA^{Trp} injected with *E. coli* activating enzyme into *Xenopus* oocytes suppresses UGA termination. *Nature* **293**, 235–237 (1981).
- Kalstrup, T. & Blunck, R. Dynamics of internal pore opening in K(V) channels probed by a fluorescent unnatural amino acid. *Proceedings of the National Academy of Sciences of the United States of America* **110**, 8272–8277, <https://doi.org/10.1073/pnas.1220398110> (2013).
- Zhu, S. *et al.* Genetically encoding a light switch in an ionotropic glutamate receptor reveals subunit-specific interfaces. *Proc Natl Acad Sci USA* **111**, 6081–6086, <https://doi.org/10.1073/pnas.1318808111> (2014).
- Nowak, M. W. *et al.* Nicotinic receptor binding site probed with unnatural amino acid incorporation in intact cells. *Science* **268**, 439–442 (1995).
- Lummiss, S. C. *et al.* Cis-trans isomerization at a proline opens the pore of a neurotransmitter-gated ion channel. *Nature* **438**, 248–252, <https://doi.org/10.1038/nature04130> (2005).
- England, P. M., Zhang, Y., Dougherty, D. A. & Lester, H. A. Backbone mutations in transmembrane domains of a ligand-gated ion channel: implications for the mechanism of gating. *Cell* **96**, 89–98 (1999).
- Santarelli, V. P., Eastwood, A. L., Dougherty, D. A., Horn, R. & Ahern, C. A. A cation-π interaction discriminates among sodium channels that are either sensitive or resistant to tetrodotoxin block. *The Journal of biological chemistry* **282**, 8044–8051, <https://doi.org/10.1074/jbc.M611334200> (2007).
- Ahern, C. A., Eastwood, A. L., Dougherty, D. A. & Horn, R. An electrostatic interaction between TEA and an introduced pore aromatic drives spring-in-the-door inactivation in Shaker potassium channels. *The Journal of general physiology* **134**, 461–469, <https://doi.org/10.1085/jgp.200910260> (2009).
- Ahern, C. A., Eastwood, A. L., Dougherty, D. A. & Horn, R. Electrostatic contributions of aromatic residues in the local anesthetic receptor of voltage-gated sodium channels. *Circ Res* **102**, 86–94, <https://doi.org/10.1161/CIRCRESAHA.107.160663> (2008).
- Pless, S. A., Galpin, J. D., Niciforovic, A. P., Kurata, H. T. & Ahern, C. A. Hydrogen bonds as molecular timers for slow inactivation in voltage-gated potassium channels. *eLife* **2**, e01289, <https://doi.org/10.7554/eLife.01289> (2013).
- Pless, S. A., Galpin, J. D., Niciforovic, A. P. & Ahern, C. A. Contributions of counter-charge in a potassium channel voltage-sensor domain. *Nature chemical biology* **7**, 617–623, <https://doi.org/10.1038/nchembio.622> (2011).

16. Lueck, J. D. *et al.* Atomic mutagenesis in ion channels with engineered stoichiometry. *Elife* **5** <https://doi.org/10.7554/eLife.18976> (2016).
17. Kim, R. Y. *et al.* Atomic basis for therapeutic activation of neuronal potassium channels. *Nature communications* **6**, 8116, <https://doi.org/10.1038/ncomms9116> (2015).
18. Saks, M. E. *et al.* An engineered Tetrahymena tRNA^{Gln} for *in vivo* incorporation of unnatural amino acids into proteins by nonsense suppression. *The Journal of biological chemistry* **271**, 23169–23175 (1996).
19. Rodriguez, E. A., Lester, H. A. & Dougherty, D. A. Improved amber and opal suppressor tRNAs for incorporation of unnatural amino acids *in vivo*. Part 1: minimizing misacylation. *RNA* **13**, 1703–1714, <https://doi.org/10.1261/rna.666807> (2007).
20. Rodriguez, E. A., Lester, H. A. & Dougherty, D. A. Improved amber and opal suppressor tRNAs for incorporation of unnatural amino acids *in vivo*. Part 2: evaluating suppression efficiency. *RNA* **13**, 1715–1722, <https://doi.org/10.1261/rna.667607> (2007).
21. Rodriguez, E. A., Lester, H. A. & Dougherty, D. A. *In vivo* incorporation of multiple unnatural amino acids through nonsense and frameshift suppression. *Proceedings of the National Academy of Sciences of the United States of America* **103**, 8650–8655, <https://doi.org/10.1073/pnas.0510817103> (2006).
22. Pless, S. A. *et al.* Asymmetric functional contributions of acidic and aromatic side chains in sodium channel voltage-sensor domains. *The Journal of general physiology* **143**, 645–656, <https://doi.org/10.1085/jgp.201311036> (2014).
23. Hao, B. *et al.* A new UAG-encoded residue in the structure of a methanogen methyltransferase. *Science* **296**, 1462–1466, <https://doi.org/10.1126/science.1069556> (2002).
24. Ibba, M. & Soll, D. Genetic code: introducing pyrrolysine. *Curr Biol* **12**, R464–466 (2002).
25. Wan, W., Tharp, J. M. & Liu, W. R. Pyrrolysyl-tRNA synthetase: an ordinary enzyme but an outstanding genetic code expansion tool. *Biochim Biophys Acta* **1844**, 1059–1070, <https://doi.org/10.1016/j.bbapap.2014.03.002> (2014).
26. Leisle, L. *et al.* Cellular encoding of Cy dyes for single-molecule imaging. *Elife* **5** <https://doi.org/10.7554/eLife.19088> (2016).
27. Sakamoto, K. *et al.* Site-specific incorporation of an unnatural amino acid into proteins in mammalian cells. *Nucleic Acids Res* **30**, 4692–4699 (2002).
28. Wang, L., Brock, A., Herberich, B. & Schultz, P. G. Expanding the genetic code of Escherichia coli. *Science* **292**, 498–500, <https://doi.org/10.1126/science.1060077> (2001).
29. Chin, J. W. Expanding and reprogramming the genetic code of cells and animals. *Annual review of biochemistry* **83**, 379–408, <https://doi.org/10.1146/annurev-biochem-060713-035737> (2014).
30. Hodgkin, A. L. & Katz, B. The effect of sodium ions on the electrical activity of giant axon of the squid. *The Journal of physiology* **108**, 37–77 (1949).
31. Hodgkin, A. L. & Huxley, A. F. A quantitative description of membrane current and its application to conduction and excitation in nerve. *J Physiol* **117**, 500–544 (1952).
32. Glynn, P. *et al.* Voltage-Gated Sodium Channel Phosphorylation at Ser571 Regulates Late Current, Arrhythmia, and Cardiac Function *In Vivo*. *Circulation* **132**, 567–577, <https://doi.org/10.1161/CIRCULATIONAHA.114.015218> (2015).
33. Guan, B., Chen, X. & Zhang, H. Two-electrode voltage clamp. *Methods Mol Biol* **998**, 79–89, https://doi.org/10.1007/978-1-62703-351-0_6 (2013).
34. Backx, P. H., Yue, D. T., Lawrence, J. H., Marban, E. & Tamaselli, G. F. Molecular localization of an ion-binding site within the pore of mammalian sodium channels. *Science* *Jl - sci* **257**, 248–251 (1992).
35. Favre, I., Moczydlowski, E. & Schild, L. On the structural basis for ionic selectivity among Na⁺, K⁺, and Ca²⁺ in the voltage-gated sodium channel. *Biophysical Journal* **71**, 3110–3125, [https://doi.org/10.1016/S0006-3495\(96\)79505-X](https://doi.org/10.1016/S0006-3495(96)79505-X) (1996).
36. Hille, B. *Ion channels of excitable membranes*. 3rd edn, (Sinauer, 2001).
37. Ambrogelly, A. *et al.* Pyrrolysine is not hardwired for cotranslational insertion at UAG codons. *Proceedings of the National Academy of Sciences of the United States of America* **104**, 3141–3146, <https://doi.org/10.1073/pnas.0611634104> (2007).
38. Pless, S. A., Galpin, J. D., Frankel, A. & Ahern, C. A. Molecular basis for class Ib anti-arrhythmic inhibition of cardiac sodium channels. *Nature communications* **2**, 351, <https://doi.org/10.1038/ncomms1351> (2011).

Acknowledgements

This work has been supported by NIH/NINDS High Impact Neuroscience Research Grant NS104617- “The facility for atomic Mutagenesis”. CAA is supported by NIH (GM106568, GM122420), is an American Heart Association Established investigator (5EIA22180002) and a member of the Membrane Protein structural Dynamics Consortium (NIH GM087519). DTI is supported by INFIEL17F0 from the Cystic Fibrosis Foundation. JDL is supported by Emily’s Entourage Foundation.

Author Contributions

D.T.I., J.D.L., and C.A.A. conceived the study, designed experiments, and wrote the paper. D.T.I., J.D.L., J.D.G., and G.D.G. conducted the experiments.

Additional Information

Supplementary information accompanies this paper at <https://doi.org/10.1038/s41598-018-23201-z>.

Competing Interests: The authors declare no competing interests.

Publisher’s note: Springer Nature remains neutral with regard to jurisdictional claims in published maps and institutional affiliations.



Open Access This article is licensed under a Creative Commons Attribution 4.0 International License, which permits use, sharing, adaptation, distribution and reproduction in any medium or format, as long as you give appropriate credit to the original author(s) and the source, provide a link to the Creative Commons license, and indicate if changes were made. The images or other third party material in this article are included in the article’s Creative Commons license, unless indicated otherwise in a credit line to the material. If material is not included in the article’s Creative Commons license and your intended use is not permitted by statutory regulation or exceeds the permitted use, you will need to obtain permission directly from the copyright holder. To view a copy of this license, visit <http://creativecommons.org/licenses/by/4.0/>.

© The Author(s) 2018